



The structure and particle size of nanocarbon liquid particle from palm oil mill effluent using the hydrothermal method

Evi Christiani Sitepu^{a*} • Gimelliya Saragih^a • Diman Raymond S. Tambunan^a • Martha Rianna^{b,c*}

^aPoliteknik Teknologi Kimia Industri, Medan 20228, Indonesia

^bUniversitas Sumatera Utara, Medan 20155, Indonesia

^cLaboratorium Fisika Komputasi, Fakultas Matematika dan Ilmu Pengetahuan Alam, Universitas Sumatera Utara, Medan 20155, Indonesia

Received 10 16 2021; accepted 10 26 2021

Available 04 30 2022

Abstract: Palm oil mill effluent (POME) is a biomass produced in a mill by processing palm oil. In this research, the structure and particle size of nanocarbon particle from palm oil mill effluent (POME) have been successfully determined by using the hydrothermal method. The characterization of structure and particle size was conducted by XRD, PSA, FTIR and UV-Vis, respectively. Single crystal of carbon structures in all peaks and an average crystal size of 30.58 nm were confirmed from XRD analysis. Then, a PSA analysis showed that the average particle sizes of nanocarbon from palm oil mill effluent were 1.153 nm. Both the analysis of structure and the analysis of particle size are indicators of nanosize from carbon particles synthesized from palm oil mill effluent. The FTIR spectrum confirmed that functional groups indicate that nanocarbons had been found in POME samples with luminescence generated from the surface state. The POME solution was successfully converted into nanocarbon in the presence of blue fluorescence under UV light and has light absorption in the UV region at a peak of ~300 nm based from the UV-Vis results.

Keywords: Palm oil mill effluent (POME), hydrothermal method, nanocarbon, particle size

*Corresponding author.

E-mail address: evsitepu@kemenperin.go.id, martharianna@usu.ac.id (Evi Christiani Sitepu, Martha Rianna).

Peer Review under the responsibility of Universidad Nacional Autónoma de México.

1. Introduction

The development of technological devices, especially in the industrial sector, is increasingly advanced where one of the applications is the use of data on industrial waste products (Vijay et al., 2016). Most of the biowaste residual from oil palm mill plantations is burned or disposed of in dumping ponds. This phenomenon causes global climate change by emitting carbon dioxide and methane gas (Awalludin et al., 2015; Sembiring et al., 2019; Utama et al., 2018). Palm oil mill effluent contains 60-83 million tons of waste, the amount of which increased by 85-110 million tons in 2020 (Onoja et al., 2019). Palm oil mill effluent has been successfully used by with natural ingredients graphene for textile Teow et al. (2019) color cleaning applications, bio-lubricant (Syaima et al., 2015) and environmental hygiene in the industrial sector (Iskandar et al., 2018).

The increasing awareness about pollution has led to the development of solutions to environmental problems by maximizing the utilization of abundant biomass for the manufacture of nanocarbons. Biomass, especially from agricultural by-products, is a rich source of cellulosic material. Biomass contains an average composition of 40%-50% cellulose, 20%-30% hemicellulose, 20%-25% lignin and 1%-5% ash and exhibits excellent water solubility, making it an attractive source of nanocarbons (Rafatullah et al., 2013). Various raw materials from biomass, including grass (Kang et al., 2005), rice husks (Muramatsu et al., 2014), coconut shells and husks (Chunduri et al., 2016), coffee beans (Jiang et al., 2014), banana leaves or peels (De & Karak, 2013), lemon peels and watermelon peels Zhou et al. (2012) have been used as carbon sources. In addition, fruit extract can be used as a carbon source and can be applied in bioimaging, as a fluorescent probe to detect Fe^{3+} ions and fluorescence ink (Zhang et al., 2018). However, the utilization of biomass from POME waste is very attractive due to the environmental friendliness of lignocellulosic material (Tanikkul et al., 2019) and its main advantages, including its abundant availability and low cost, make this biomass a suitable precursor for nanocarbon manufacture.

Nanocarbon is a semiconductor nanocrystalline material that has a diameter smaller than 10 nanometers which has good photostability, high water solubility, and its chemical properties are easy to modify. Then, the hydrothermal method is an effective method for making carbonization and can make materials in nanosize (Abbas et al., 2018). The manufacture of nanocarbons has been widely carried out using the hydrothermal method from rice husks (Sun & Lei, 2017), then fluorescent nanocarbon using the hydrothermal method from fruit extracts for catalyst applications (Arul et al., 2017).

We performed the research on the synthesis of the nanocarbon particle from palm oil mill effluent using a hydrothermal method. The characterization of the structure and particle size distribution using XRD and PSA is presented.

2. Materials and methods

Palm oil mill effluent solution was collected from palm oil in Sumatera Utara, Indonesia. Palm oil mill effluent solution as precursor of 100 g was added to 1000 ml of distilled water and centrifuged for 60 seconds at 3000 rpm for 3 times. Furthermore, the precursor was centrifuged and stirred on a hotplate for 30 minutes at room temperature. The solution was poured into a Teflon tube and put in an oven heated at 200°C for 6 hours. After cooling, the nanocarbon solution was centrifuged at 3000 rpm for 60 seconds and the supernatant solution was filtered using a dialysis membrane (0.45 μ m nylon) dipped in distilled water for 24 hours. To evaluate the properties of the sample developed in this study, structural and particle size characterizations were performed by X-ray diffraction analysis (XRD), particle size analyzer (PSA), Fourier Transform Infrared (FT-IR) spectroscopy and UV-Vis spectroscopy.

3. Results and discussion

The X-ray diffraction (XRD) analysis of the nanocarbon particle from palm oil mill effluent is shown in Figure 1. For the evaluation of degree in the nanocarbon particle from palm oil mill effluent, also called crystallized structured in PF nanocomposites, the XRD profile of sample was used as a reference. According to the XRD results, the absence of a peak in the XRD pattern indicated that the nanocarbon particle from palm oil mill effluent was a crystalline structure with the variations of carbon.

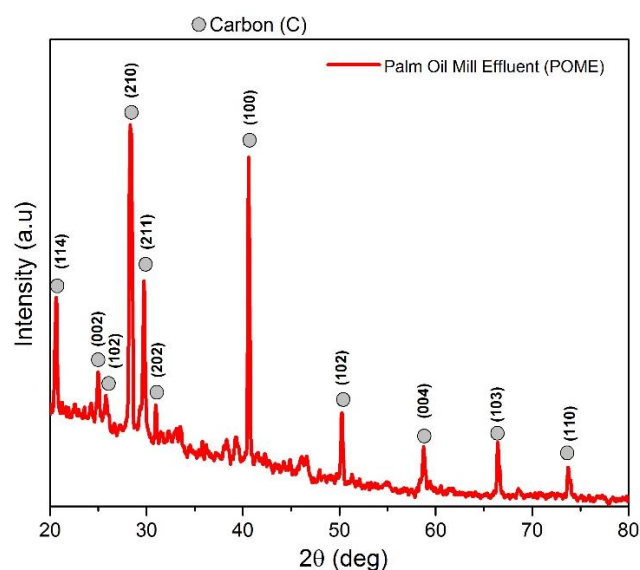


Figure 1. XRD pattern of nanocarbon from palm oil mill effluent.

Figure 1 shows structural of nanocarbon from palm oil mill effluent. In Figure 1, the peak of nanocarbon can be seen in (hkl) of (114), (002), (102), (210), (211), (202), (100), (102), (004), (103), (110). XRD pattern in Figure 1 confirmed carbon structures in all peaks. The results are the same as those reported by Howe et al. (2003) that carbon structures observed in 002 and 102, among others. The parameters of the crystal sample nanocarbon from palm oil mill effluent in all crystal planes can be seen in Table 1.

Table 1. Parameters of the crystal sample nanocarbon from palm oil mill effluent in all crystal planes.

Peak	2 θ (deg.)	hkl	FWHM (deg.)	D (nm)
1	20.74	114	0.31	26.91
2	25.01	002	0.24	34.76
3	25.97	102	0.22	37.93
4	28.33	210	0.41	20.35
5	29.87	211	0.29	28.77
6	31.07	202	0.19	43.91
7	40.54	100	0.24	34.76
8	50.51	102	0.25	33.37
9	58.82	004	0.22	37.92
10	66.40	103	0.53	15.74
11	73.28	110	0.38	21.95

In Table 1, the peaks list increases with FWHM but it decreases with crystal size (D). This research shows that the XRD pattern can be provide information about impurity of nanocarbon from palm oil mill effluent synthesized using the hydrothermal method. As seen in Figure 1, some peaks confirmed the other carbon unsure. Generally, the palm oil mill effluent has amorphous structures. The results of the amorphous structure from nanocarbon is also confirmed from previous results with a precursor of citric acid (Hu et al., 2017; Bhisare et al., 2015; Takayanagi et al., 2020). However, in this research, making palm oil mill effluent by using the hydrothermal method could confirm that carbon unsure from Figure 1.

Figure 2 shows the particle size distribution of nanocarbon from palm oil mill effluent using a particle size analyzer (PSA) with a hydrothermal method. The average particle size of nanocarbon from palm oil mill effluent in Figure 2 was 1.153 nm.; whereas the average crystal size sown in Table 1 was 30.58 nm. These results showed that synthesized carbon particle from palm oil mill effluent using the hydrothermal method was successfully in nanosize. The particle size of nanocarbon increases because of the measurement of the hydrodynamic diameter of a nanocarbon containing a hydrophilic functional group on the surface of nanocarbon (Wu et al., 2017; Yang et al., 2011).

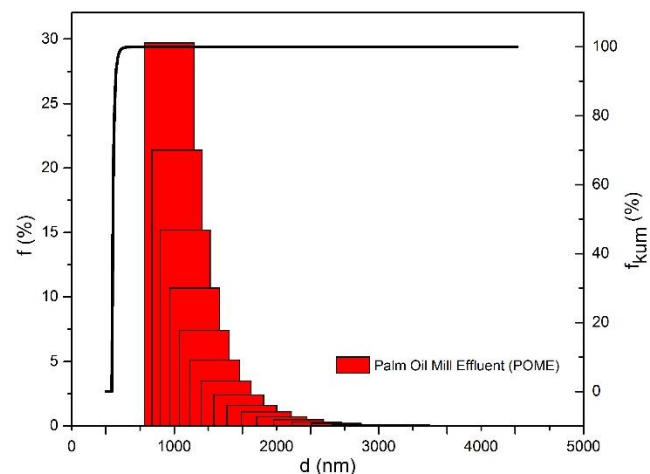


Figure 2. Particle size distribution of nanocarbon from palm oil mill effluent.

The FTIR results from nanocarbon synthesized through a hydrothermal process are shown in Figure 3.

In Figure 3, the wave numbers of 3332 cm^{-1} confirmed for O-H and N-H groups, while the wave number of 2838 and 2949 cm^{-1} confirmed for C-H vibrational groups (Gong et al., 2019). Correspondingly, at wave number of 1645 cm^{-1} is the bending vibrational group of N-H, where at wave number of 1014 and 1409 cm^{-1} can be considered as stretching asymmetry and symmetry of the C-O-C group which is a functional group of nanocarbon (Bu et al., 2019). The results of the nanocarbon FTIR obtained are also similar to the results of the nanocarbon FTIR obtained from coal as reported by Purwandari et al. (2020). The above functional groups indicate that nanocarbons have been found in POME samples with luminescence generated from the surface state.

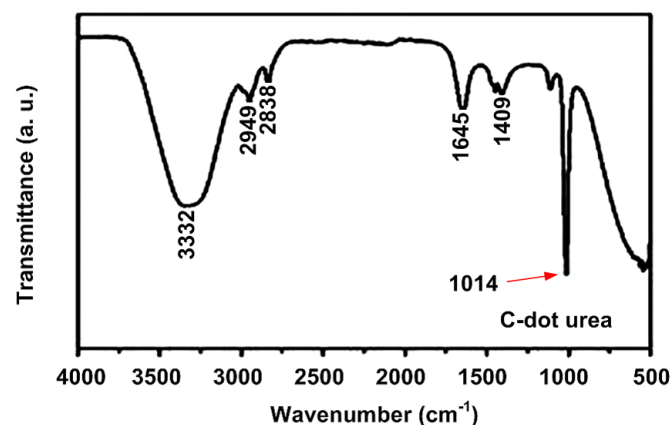


Figure 3. FTIR spectrum of nanocarbon from palm oil mill effluent.

The absorption of nanoscale carbon from a wavelength of 280 - 400 nm with the absorption peak at the peak of 300 nm. The results of the UV-Vis spectrum show that the POME solution has been successfully converted into nanocarbon in the presence of blue fluorescence under UV light and has light absorption in the UV region at a peak of ~300 nm. This peak indicates the transition peak of the aromatic bond by C=C of nanocarbon (Ansi et al., 2021). The results of this absorption spectrum are also similar to previous studies for the conversion of food waste to carbon dot with an absorption spectrum at a peak of around 300 nm (Gan et al., 2020; Zhou et al., 2018).

4. Conclusions

Based on the XRD analysis crystals of carbon structures in all peaks and an average crystal size of 30.58 nm were found. The PSA analysis showed that the average particle sizes of nanocarbons from palm oil mill effluent was 1.153 nm. The FTIR spectrum confirmed that the functional groups indicate that nanocarbon have been found in POME samples with luminescence generated from the surface state. The POME solution was successfully converted into nanocarbon in the presence of blue fluorescence under UV light and has a light absorption in the UV region at a peak of ~300 nm based on the UV-Vis results.

Conflict of interest

The author(s) does/do not have any type of conflict of interest to declare.

Acknowledgments

The authors would like to thank the Ministry of Industrial Republic of Indonesia and Universitas Sumatera Utara for the partial support provided for this research.

Financing

The authors did not receive any sponsorship to carry out the research reported in the present manuscript.

References

- Abbas, A., Mariana, L. T., & Phan, A. N. (2018). Biomass-waste derived graphene quantum dots and their applications. *Carbon*, *140*, 77-99. <https://doi.org/10.1016/j.carbon.2018.08.016>
- Ansi V. A., Ritu G., Thasleena Panakkal, Aji A. Anappara & Renuka N. K. (2021). Acetic acid derived carbon dots as efficient pH and bio-molecule sensor. *International Journal of Environmental Analytical Chemistry*, *101*(4), 506-512. <https://doi.org/10.1080/03067319.2019.1669581>
- Arul, V., Edison, T. N. J. I., Lee, Y. R., & Sethuraman, M. G. (2017). Biological and catalytic applications of green synthesized fluorescent N-doped carbon dots using *Hylocereus undatus*. *Journal of Photochemistry and Photobiology B: Biology*, *168*, 142-148. <https://doi.org/10.1016/j.jphotobiol.2017.02.007>
- Awalludin, M. F., Sulaiman, O., Hashim, R., & Nadhari, W. N. A. W. (2015). An overview of the oil palm industry in Malaysia and its waste utilization through thermochemical conversion, specifically via liquefaction. *Renewable and Sustainable Energy Reviews*, *50*, 1469-1484. <https://doi.org/10.1016/j.rser.2015.05.085>
- Bhaisare, M. L., Talib, A., Khan, M. S., Pandey, S., & Wu, H. F. (2015). Synthesis of fluorescent carbon dots via microwave carbonization of citric acid in presence of tetraoctylammonium ion, and their application to cellular bioimaging. *Microchimica Acta*, *182*(13), 2173-2181. <https://doi.org/10.1007/s00604-015-1541-5>
- Bu, L., Luo, T., Peng, H., Li, L., Long, D., Peng, J., & Huang, J. (2019). One-step synthesis of N-doped carbon dots, and their applications in curcumin sensing, fluorescent inks, and super-resolution nanoscopy. *Microchimica Acta*, *186*(10), 1-12. <https://doi.org/10.1007/s00604-019-3762-5>
- Chunduri, L. A., Kurdekar, A., Patnaik, S., Dev, B. V., Rattan, T. M., & Kamiseti, V. (2016). Carbon quantum dots from coconut husk: evaluation for antioxidant and cytotoxic activity. *Materials Focus*, *5*(1), 55-61. <https://doi.org/10.1166/mat.2016.1289>
- De, B., & Karak, N. (2013). A green and facile approach for the synthesis of water soluble fluorescent carbon dots from banana juice. *Rsc Advances*, *3*(22), 8286-8290. <https://doi.org/10.1039/C3RA00088E>
- Gan, Y. X., Jayatissa, A. H., Yu, Z., Chen, X., & Li, M. (2020). Hydrothermal Synthesis of Nanomaterials. *Journal of Nanomaterials*, *2020*, 1-3. <https://doi.org/10.1155/2020/8917013>

- Gong, P., Sun, L., Wang, F., Liu, X., Yan, Z., Wang, M., ... & You, J. (2019). Highly fluorescent N-doped carbon dots with two-photon emission for ultrasensitive detection of tumor marker and visual monitor anticancer drug loading and delivery. *Chemical Engineering Journal*, 356, 994-1002. <https://doi.org/10.1016/j.cej.2018.09.100>
- Howe, J. Y., Rawn, C. J., Jones, L. E., & Ow, H. (2003). Improved crystallographic data for graphite. *Powder diffraction*, 18(2), 150-154. <https://doi.org/10.1154/1.1536926>
- Hu, Q., Gong, X., Liu, L., & Choi, M. M. (2017). Characterization and analytical separation of fluorescent carbon nanodots. *Journal of Nanomaterials*, vol. 2017, 1-23. <https://doi.org/10.1155/2017/1804178>
- Iskandar, M. J., Baharum, A., Anuar, F. H., & Othaman, R. (2018). Palm oil industry in South East Asia and the effluent treatment technology—A review. *Environmental technology & innovation*, 9, 169-185. <https://doi.org/10.1016/j.eti.2017.11.003>
- Jiang, C., Wu, H., Song, X., Ma, X., Wang, J., & Tan, M. (2014). Presence of photoluminescent carbon dots in Nescafe® original instant coffee: applications to bioimaging. *Talanta*, 127, 68-74. <https://doi.org/10.1016/j.talanta.2014.01.046>
- Kang, Z., Wang, E., Mao, B., Su, Z., Chen, L., & Xu, L. (2005). Obtaining carbon nanotubes from grass. *Nanotechnology*, 16(8), 1192-1195.
- Muramatsu, H., Kim, Y. A., Yang, K. S., Cruz-Silva, R., Toda, I., Yamada, T., ... & Saitoh, H. (2014). Rice husk-derived graphene with nano-sized domains and clean edges. *Small*, 10(14), 2766-2770. <https://doi.org/10.1002/smll.201400017>
- Onoja, E., Chandren, S., Abdul Razak, F. I., Mahat, N. A., & Wahab, R. A. (2019). Oil palm (*Elaeis guineensis*) biomass in Malaysia: The present and future prospects. *Waste and Biomass Valorization*, 10(8), 2099-2117. <https://doi.org/10.1007/s12649-018-0258-1>
- Purwandari, V., Gea, S., Wirjosentono, B., Haryono, A., Mahendra, I. P., & Hutapea, Y. A. Electrical and Thermal Conductivity of Cyclic Natural Rubber/Graphene Nanocomposite Prepared by Solution Mixing Technique. *Indonesian Journal of Chemistry*, 20(4), 801-809. <https://doi.org/10.22146/ijc.44791>
- Rafatullah, M., Ahmad, T., Ghazali, A., Sulaiman, O., Danish, M., & Hashim, R. (2013). Oil palm biomass as a precursor of activated carbons: a review. *Critical reviews in environmental science and technology*, 43(11), 1117-1161. <https://doi.org/10.1080/10934529.2011.627039>
- Sembiring, T., Sitepu, E., Rianna, M., Warman, A., Sinuhaji, P., & Sebayang, K. (2019). Fabrication and characterization of palm sugar tree (*Arenga pinnata*) fiber composites reinforced by polyester resin. *Functional materials*, 26, 121-126. <https://doi.org/10.15407/fm26.01.121>
- Sun, X., & Lei, Y. (2017). Fluorescent carbon dots and their sensing applications. *TrAC Trends in Analytical Chemistry*, 89, 163-180. <https://doi.org/10.1016/j.trac.2017.02.001>
- Syaima, M. T. S., Ong, K. H., Noor, I. M., Zamratul, M. I. M., Brahim, S. A., & Hafizul, M. M. (2015). The synthesis of bio-lubricant based oil by hydrolysis and non-catalytic of palm oil mill effluent (POME) using lipase. *Renewable and Sustainable Energy Reviews*, 44, 669-675. <https://doi.org/10.1016/j.rser.2015.01.005>
- Takayanagi, T., Iwasaki, S., Becchaku, Y., Yabe, S., Morita, K., Mizuguchi, H., & Hirayama, N. (2020). Capillary Electrophoretic Characterization of Water-soluble Carbon Nanodots Formed from Glutamic Acid and Boric Acid under Microwave Irradiation. *Analytical Sciences*, 36(8), 941-946. <https://doi.org/10.2116/analsci.19P484>
- Tanikkul, P., Boonyawanich, S., He, M., & Pisutpaisal, N. (2019). Thermophilic biohydrogen recovery from palm oil mill effluent. *International Journal of Hydrogen Energy*, 44(11), 5176-5181. <https://doi.org/10.1016/j.ijhydene.2018.10.005>
- Teow, Y. H., Nordin, N. I., & Mohammad, A. W. (2019). Green synthesis of palm oil mill effluent-based graphenic adsorbent for the treatment of dye-contaminated wastewater. *Environmental Science and Pollution Research*, 26(33), 33747-33757. <https://doi.org/10.1007/s11356-018-2189-6>
- Utama, P. S., Yamsaengsung, R., & Sangwichien, C. (2018). Silica gel derived from palm oil mill fly ash. *Songklanakarin Journal Science and Technology*, 40(1), 121-126.
- Vijay, V., Pimm, S. L., Jenkins, C. N., & Smith, S. J. (2016). The impacts of oil palm on recent deforestation and biodiversity loss. *PloS one*, 11(7), 1-19. <https://doi.org/10.1371/journal.pone.0159668>
- Wu, P., Li, W., Wu, Q., Liu, Y., & Liu, S. (2017). Hydrothermal synthesis of nitrogen-doped carbon quantum dots from microcrystalline cellulose for the detection of Fe³⁺ ions in an acidic environment. *RSC advances*, 7(70), 44144-44153. <https://doi.org/10.1039/C7RA08400E>

Yang, Z. C., Li, X., & Wang, J. (2011). Intrinsically fluorescent nitrogen-containing carbon nanoparticles synthesized by a hydrothermal process. *Carbon*, 49(15), 5207-5212.

<https://doi.org/10.1016/j.carbon.2011.07.038>

Zhang, S., Sui, L., Dong, H., He, W., Dong, L., & Yu, L. (2018). High-performance supercapacitor of graphene quantum dots with uniform sizes. *ACS applied materials & interfaces*, 10(15), 12983-12991.

<https://doi.org/10.1021/acsami.8b00323>

Zhou, J., Sheng, Z., Han, H., Zou, M., & Li, C. (2012). Facile synthesis of fluorescent carbon dots using watermelon peel as a carbon source. *Materials Letters*, 66(1), 222-224.

<https://doi.org/10.1016/j.matlet.2011.08.081>

Zhou, Y., Liu, Y., Li, Y., He, Z., Xu, Q., Chen, Y., ... & Nelles, M. (2018). Multicolor carbon nanodots from food waste and their heavy metal ion detection application. *RSC advances*, 8(42), 23657-23662.